Crustal thickness variation in south-central Alaska

Elizabeth Veenstra
Douglas H. Christensen
Geophysical Institute, University of Alaska Fairbanks, Fairbanks, Alaska 99775-7320, USA
Geoffrey A. Abers
Aaron Ferris
Department of Earth Sciences, Boston University, Boston, Massachusetts 02215, USA

ABSTRACT

Crustal thicknesses have been determined by receiver function analysis of broadband teleseismic waveforms recorded during the Broadband Experiment Across the Alaska Range (BEAAR). Typical crust beneath the northern lowlands is 26 km thick, while beneath the mountains it is 35–45 km thick. The transition from thick to thin crust coincides with the location of the Hines Creek fault, a major tectonostratigraphic boundary. Crustal thicknesses determined by receiver functions agree with those predicted from topography assuming Airy type isostasy, suggesting that the Alaska Range is compensated by its crustal root. North of the range, however, the crust is systematically thinner than predicted by simple Airy isostasy. A crustal density contrast of 4.6% across the Hines Creek fault, 2700 kg m^{-3} to the north and 2830 kg m^{-3} to the south, explains the observed difference between the crustal thicknesses predicted by simple Airy isostasy, and the crustal thicknesses determined by receiver function analysis.

Keywords: Alaska Range, crust, PASSCAL, Mohorovicic discontinuity, isostasy, teleseismic signals.

INTRODUCTION

Continental deformation and wide plate boundary zones represent a departure from the simple rigid plate model of plate tectonics. In addition, the relative importance of dynamic and structural mechanisms of uplift above subduction zones is not well understood. Numerical experiments suggest that topography above subduction zones is due to plate coupling and the transmission of horizontal stress (England and McKenzie, 1982). Other studies suggest that topography above subduction zones results from dynamic forces acting on the base of the crust (Melosh and Raefsky, 1980). Observations of crustal thickness may help us discriminate between dynamic models to provide a better understanding of how mountains are supported.

South-central Alaska is a geologically complex and tectonically active region of accreted tectonostratigraphic terranes and dispersed and translated fragments of North American continental crust (Nokleberg et al., 1994). South-central Alaska overrides a shallow subduction zone, where the North American–Pacific plate boundary undergoes a transition from transform to convergent motion. Described as a closed corner transition (Mann and Frohlick, 1999), the Alaska Range forms the corner far inland, rising to 6194 m (Mount McKinley, the highest peak in North America). Apatite fission track thermochronology and geologic evidence indicate that surface uplift began ca. 5–6 Ma (Fitzgerald et al., 1995). The curvilinear Alaska Range is split by the seismically active Denali fault system, a 1200-km-long dominantly right-lateral strike-slip fault system, responsible for the Mw 7.9 earthquake on 3 November 2002 (Eberhart-Phillips et al., 2003). Active seismicity of the Aleutian Wadati-Benioff zone disappears to the east beneath the Alaska Range, as does active arc volcanism. Tectonic affinities of terranes along the Broadband Experiment Across the Alaska Range (BEAAR) transect range from metamorphosed continental margin to turbidite basins to displaced volcanic arcs (Plafker and Berg, 1994). The configuration of mountains, major thrust and strike-slip faults, and tectonic affinities of terranes all evidence the transpressional environment of southern Alaska.

The Trans-Alaska Crustal Transect (TACT) seismic refraction profile (Page et al., 1986; Beaudoin et al., 1992, 1994) crossed the eastern edge of the Alaska Range along the Richardson Highway, where crust is reported to be 50 km thick at the Denali fault and as thin as 28 km north of the range (Brocher et al., 2004). The BEAAR project examined crustal structure beneath the central Alaska Range along the Parks Highway, and here we present crustal thicknesses determined by receiver function analysis. These crustal thickness data provide an important constraint for hypotheses on tectonic evolution of Alaska, where geological and geophysical differences between tectonostratigraphic terranes are incompletely documented.

RECEIVER FUNCTION ANALYSIS

We deployed 36 three-component broadband seismic stations (Fig. 1A), and collected high-quality data over a period of 27 months. A three-phase deployment used broadband Guralp sensors (22 CMG3T and 14 CMG3ESP seismometers) and Reftek recorders. Phase one began May 1999 with 7 stations at ~50 km spacing. Phase two began May 2000 with deployment of an additional 29 stations at ~10 km spacing along the main line. Phase three began September 2000 with half of the instrumentation arranged in a sparser network. The continuously recording data stream with 50 samples/s was decimated to 6.25 samples/s for receiver function analysis.

Receiver function analysis measures crustal structure in the vicinity of three-component broadband seismic stations (Langston, 1979). An incident teleseismic P wave produces converted phases at discrete boundaries beneath the station, the large impedance contrast at the crust-mantle boundary generating a prominent P-to-S conversion (Ps). These phases can be separated from the incident source pulse by deconvolution. North-south and east-west components of ground motion are rotated into radial and tangential components. In horizontally layered structure, all S wave motion at

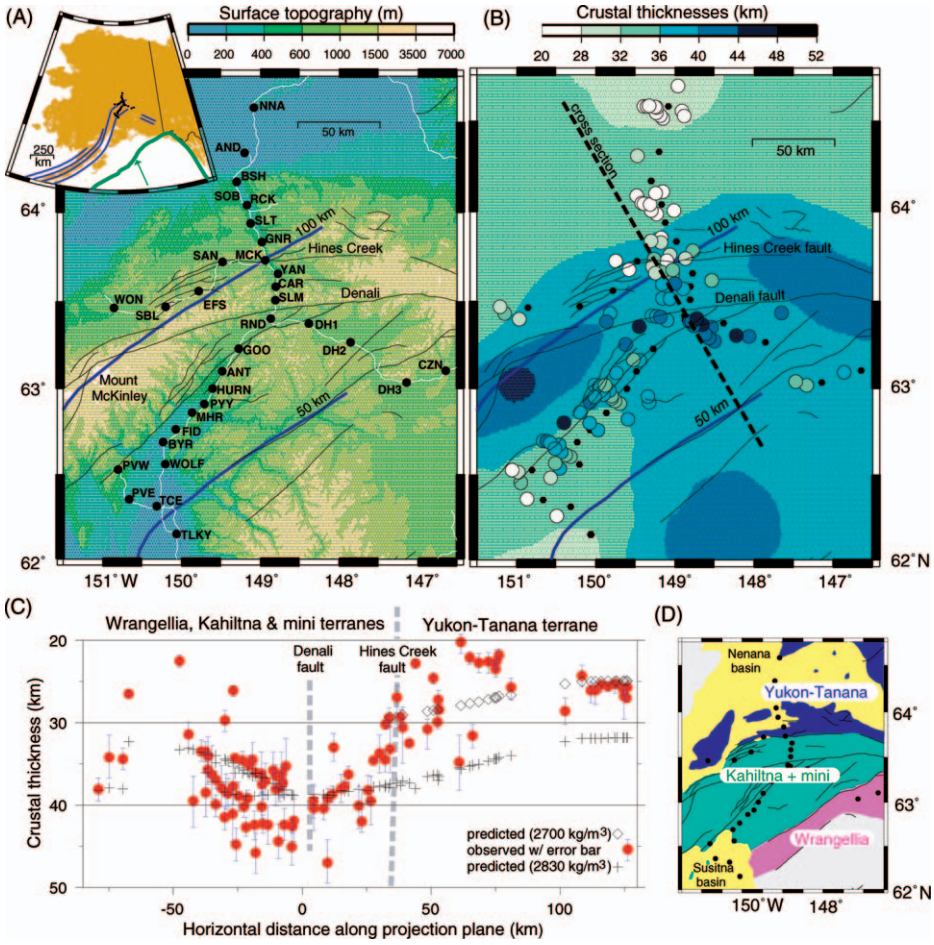

Figure 1. A, inset: Plate boundary map. South-central Alaska overrides shallow-dipping subduction zone, where North American–Pacific plate boundary undergoes transition from transform to convergent motion. Map locates transect, Pacific plate motion vector, and Wadati-Benioff zone 50, 100, 150, and 200 km depth contours. A: Broadband Experiment Across the Alaska Range (BEAAR) station location map: 50 and 100 km slab seismicity contours (thick lines), roads (white), and mapped faults (thin black), plotted over surface topography. B: Crustal thickness results: BEAAR data (circles) plotted at latitude and longitude of Moho piercing point with crustal thickness predicted from topography assuming Airy isostasy (background). Dashed line indicates projection plane for cross section. Color contrast between data circles and background indicate discrepancy between BEAAR data and predicted crustal thickness (homogeneous crustal density 2830 kg m^{-3}). North of range data points indicate crust is thinner than predicted. C: Projected cross section: BEAAR data (dots) and crustal thickness predicted from topography projected onto vertical plane through station RND with azimuth 330°. Projection plane is orthogonal to local strike of Alaska Range. Horizontal axis indicates distance from RND, positive to north-northwest. Blue bars represent 95% confidence interval for each crustal thickness estimate. Scatter is in part due to projection of widely scattered data points onto single plane, seen by comparison with map view. Observed variation in crustal thickness (dots; >20 km) is much larger than variation in crustal thickness predicted by Airy isostasy (crosses; <10 km). D: Simplified terrane map (after Silberling et al., 1994).

the point of conversion is in the direction of the radial component. Deconvolution of the vertical component from the radial and tangential components removes instrument, source, and external path effects, thereby isolating the receiver function (Owens et al., 1984). BEAAR receiver functions were calculated using frequency domain deconvolution.

Of the 995 global events with moment magnitudes (Mw) ≥ 5.5 during the BEAAR deployment, 751 were between 29° and 101° from centrally located station RND. These teleseismic events yielded 14,754 three-component seismograms. We rejected 6644 raw seismograms and 7021 receiver functions, mainly due to inferior signal-to-noise ratios.

Individual receiver functions at each station were grouped based on similar back-azimuth and distance as well as trace similarity. Each group of receiver functions was stacked to improve the signal-to-noise ratio, and an average back-azimuth and distance calculated. Mohorovicic discontinuity (Moho) depths are determined by fitting 20 s of a stacked receiver function to a simple plane layered model with a crustal P velocity (V_p) = 6.5 km/s, a V_p/V_s ratio of 1.73 (V_s is S wave velocity), and a mantle P velocity of 8.2 km/s (McNamara and Pasyanos, 2002; Zhao et al., 1995; Wolf et al., 1991; Beaudoin et al., 1992, 1994), minimizing root-mean-square misfit between data and synthetics, similar to Sheehan et al. (1995). An F test is used to generate confidence limits on a fully nonlinear grid search (see Ferris et al., 2003). Each stack provides one crustal thickness estimate. The lateral offset of the Moho piercing point was determined for each stack. The lateral offset is given by: $X_s = h\tan[\mathrm{asin}(pV_s)]$, where h is the crustal thickness (in km) and p is the ray parameter (in s/km; V_s is in km/s).

The fit between a stacked waveform and the modeled waveform provided further quality control (Fig. 2). We eliminated 36 crustal thickness estimates due to multiple lows in the root-mean-square misfit curve, indicating a complicated waveform or an indistinct Ps conversion. Complicated waveforms can be produced by geologic structures such as faults and folds, common in the Alaska Range. An additional 29 crustal thickness estimates were eliminated because the 95% confidence interval (blue bar, Fig. 1C) was ≥7.0 km. The remaining 106 crustal thickness estimates are presented in Figures 1B and 1C.

Sedimentary basins significantly affect a seismic waveform by delaying and broadening the main pulse (Fig. 2C). This was observed north of the mountains at stations AND, BSH, SOB, RCK, SLT, and SAN, as well as to the south at PVE, TCE, and TLKY. To account for sedimentary basins in receiver function modeling, we employed a double grid search with two interfaces. The uppermost interface was allowed to vary between 0 and 5 km depth, representing the base of a sedimentary unit given a compressional velocity of 3.3 km/s and V_p/V_s of 1.97 (Castagna et al., 1985), while the lower interface represented the Moho. The compressional velocity was chosen to be representative of sedimentary units, and the V_p/V_s was determined using Pickett's mudrock trend, $V_p = 1.16V_s + 1.36$ (Ludwig et al., 1970; Castagna et al., 1985), comparable to those determined by Brocher (2005). Modeled basin thicknesses of 0.9–1.5 km were in reasonable agreement with available geologic data (Kirschner, 1994; Csejtey et al., 1992).

RESULTS AND DISCUSSION

The crustal thicknesses determined by modeling receiver functions calculated from BEAAR seismograms indicate a shallow Moho north of the Alaska Range, and a deep,

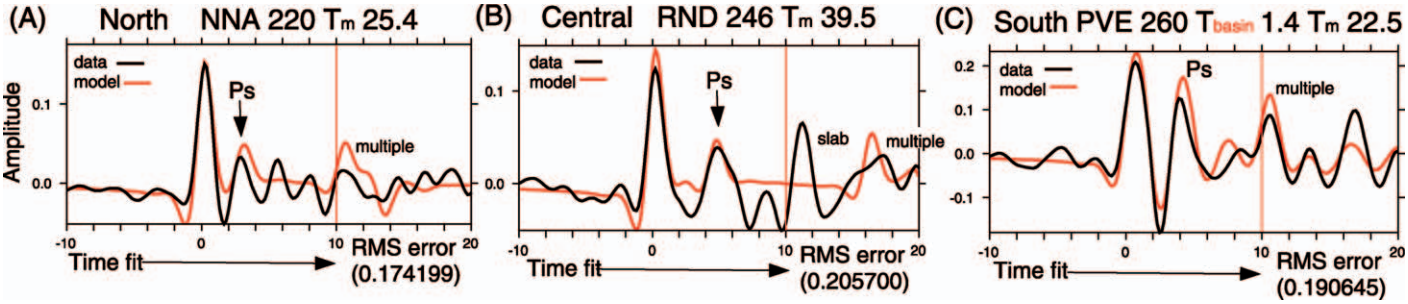

Figure 2. A–C: Sample receiver functions show fit between stacked waveform and modeled waveform at three locations. Moho depth is determined by minimizing misfit between observed (black) and calculated (red) waveforms, to thin vertical line. We do not attempt to fit multiples because those arrivals are significantly affected by nonhorizontal boundaries. Shallow sedimentary basins significantly affect waveform, and must be included in model, as at southern station PVE. RMS—root mean square.

irregular Moho in the central Alaska Range. Typical crust north of the range is 26 km thick, while beneath the central Alaska Range it is 35–45 km thick (Figs. 1B, 1C).

These crustal thickness data allow us to consider isostatic compensation of the Alaska Range. Assuming perfect Airy isostasy we compare crustal thickness predicted from topography to crustal thickness determined by receiver function analysis. We use a mean crustal density of 2830 kg m^{-3} (Christensen and Mooney, 1995), a crust/mantle density contrast of 470 kg m^{-3}, and a background crustal thickness of 31 km to predict the thickness of an isostatically compensated crust. These parameters were determined by a complete search varying smoothing, background crustal thickness, and density contrast to determine the best fit to the observed data. We smooth topography to eliminate short wavelength components, averaging elevation with 60 km radius around each point to predict crustal thickness. Crustal thicknesses determined by receiver function analysis are shown with crustal thicknesses predicted from topography in Figures 1B and 1C. In addition to an Airy model, we also considered a flexural model for isostatic compensation, in which the crust floats buoyantly on an elastic layer that spreads topographic load over a broader region. The flexural model produced results similar to the Airy model with smoothed topography.

Crustal thickness estimates vary largely within an overall pattern of thin crust to the north and thick crust beneath the mountains; those variations are concentrated at the transitions between lowlands and mountains (Fig. 1B). Beneath the Alaska Range observed crustal thicknesses are comparable to those predicted by the isostatic model, while beneath the northern foothills and lowlands, the crust is thinner than predicted from topography. Observations indicate a transition from thick to thin crust near station MCK.

The disparity between thick crust beneath the mountains and thin crust to the north suggests a fundamental change in material properties or mode of compensation. This change may be associated with geophysical disparities between terranes. To the north is metamorphosed continental margin, Yukon-Tanana; to the south is deep marine and island arc, Kahiltna and Wrangellia (Fig. 1D). Smaller terranes are interspersed near the margin (Windy, Broad Pass, Chilitna, Susitna, West Fork, McKinley, Pingston, and Nenana) (Silberling et al., 1994).

Comparison between observed crustal thicknesses and those predicted by the isostatic model indicates that the Alaska Range is isostatically compensated by the crustal root. Beneath the northern foothills and lowlands the crust is thinner than predicted by our simple isostatic model, suggesting that a simple Airy model alone is inadequate. If we assume that the region is in isostatic equilibrium, as suggested by the isostatic gravity map of Alaska (Barnes et al., 1994), the crust beneath this area must be compensated through other means, such as crustal or mantle density variations. If we assume mean crustal density beneath the northern lowlands of 2700 kg m^{-3}, then predicted crustal thicknesses are much closer to our observed values. Although lateral density variations are not allowed in an Airy model, an average crustal density of 2700 kg m^{-3} to the north and an average crustal density of 2830 kg m^{-3} to the south would explain our data, and seem reasonable given the lithologic contrast between the metamorphosed continental margin rocks north of the Hines Creek fault and deep marine and island arc rocks to the south (Ludwig et al., 1970; Brocher et al., 2004).

Our crustal thickness results are similar to TACT results in the eastern Alaska Range, ~150–200 km east of our study, which found 22 km relief between northern lowlands and the eastern Alaska Range (Brocher et al., 2004). Ai et al. (2005) examined BEAAR waveform data, reporting 24 crustal thicknesses ranging from 26.0 to 42.6 km, similar to our preliminary studies (Meyers et al., 2000, 2001, 2002). Crustal thickness variation across the Alaska Range, ~20 km, is larger than the variation observed in a similar experiment across the Colorado Rocky Mountains. Crustal thickness beneath the Colorado Rocky Mountains is only 7 km greater than that beneath the Great Plains (Sheehan et al., 1995). The transition in crustal thickness north of the Alaska Range coincides with a major tectonostratigraphic boundary. Sharp changes in Moho depth have been noted elsewhere, such as the southern edge of the Qaidam Basin in Tibet, a major boundary with a Moho offset of 15–20 km (Zhu and Helmberger, 1998).

The relief at the base of the crust does not appear to be due to a warm, buoyant mantle, as the boundary between low and high seismic attenuation regions is 30–50 km southeast of our observed boundary (Stachnik et al., 2004), and it is unlikely to be associated with the subducting slab, which appears to extend well north of our observed boundary (Ferris et al., 2003). If the northern lowlands are in isostatic equilibrium, then there must be a change in material properties across the Hines Creek fault. It seems reasonable to expect some difference in material properties across an accretionary suture where metamorphosed continental margin rocks meet deep marine and island arc rocks. A crustal density contrast across the Hines Creek fault, 2700 kg m^{-3} to the north and 2830 kg m^{-3} to the south, explains the difference between the crustal thicknesses predicted by simple Airy isostasy, and the crustal thicknesses determined by receiver function analysis.

Our results indicate that variations in both crustal thickness and density are required to explain the seismic and gravity data. Thin crust beneath the northern lowlands supports proposed tectonic extension of the Yukon-Tanana terrane (Pavlis et al., 1993). Crustal thicknesses across the central Alaska Range suggest that these mountains are supported by a crustal root developed ca. 5–6 Ma due to transmission of horizontal stress.

ACKNOWLEDGMENTS

This work benefited from contributions by many individuals, including intense physical labor during the field deployment. Instrumentation was provided by the Program for the Array Seismic Studies of the Crustal Lithosphere of the Incorporated Research Institutions for Seismology. We thank friends at the Alaska Earthquake Information Center for field assistance, and University of Alaska Fairbanks Office of Land Management personnel for assistance obtaining land use permits. Figures were made using the Generic Mapping Tool of Wessel and Smith (1995). We also thank T.M. Brocher, W.D. Mooney, D. McNamara, L. Wolf, and S.A.P.L. Cloetingh for helpful reviews. The National Science Foundation supported the Broadband Experiment Across the Alaska Range with grant EAR-9725168.

REFERENCES CITED

Ai, Y., Zhao, D., Gao, X., and Xu, W., 2005, The crust and upper mantle discontinuity structure beneath Alaska inferred from receiver functions: Physics of the Earth and Planetary Interiors, v. 150, p. 339–350, doi: 10.1016/j.pepi.2004.12.002.

Barnes, D.F., Mariano, J., Morin, R.L., Roberts, C.W., and Jachens, R.C., 1994, Incomplete isostatic gravity map of Alaska, *in* Plafker, G., and Berg, H.D., eds., The geology of Alaska: Boulder, Colorado, Geological Society of America, Geology of North America, v. G-1, plate 9, scale 1:2,500,000.

Beaudoin, B.C., Fuis, G.S., Mooney, W.D., Nokleberg, W.J., and Christensen, N.I., 1992, Thin, low-velocity crust beneath the southern Yukon-Tanana terrane, east central Alaska: Results from Trans-Alaska Crustal Transect refraction/wide-angle reflection data: Journal of Geophysical Research, v. 97, no. B2, p. 1921–1942.

Beaudoin, B.C., Fuis, G.S., Lutter, W.J., Mooney, W.D., and Moore, T.E., 1994, Crustal velocity structure of the northern Yukon-Tanana upland, central Alaska: Results from TACT refraction/wide-angle reflection data: Geological Society of America Bulletin, v. 106, p. 981–1001, doi: 10.1130/0016-7606(1994)106<0981:CVSOTN>2.3.CO;2.

Brocher, T.M., 2005, Empirical relations between elastic wavespeeds and density in the Earth's crust: Seismological Society of America Bulletin, v. 95, p. 2081–2092.

Brocher, T.M., Fuis, G.S., Lutter, W.J., Christensen, N.I., and Ratchovski, N.A., 2004, Seismic velocity models for the Denali fault zone along the Richardson Highway, Alaska: Bulletin of the Seismological Society of America, v. 94, no. 6B, p. S85–S106.

Castagna, J.P., Batzle, M.L., and Eastwood, R.L., 1985, Relationships between compressional-wave and shear-wave velocities in clastic silicate rocks: Geophysics, v. 50, p. 571–581, doi: 10.1190/1.1441933.

Christensen, N.K., and Mooney, W.D., 1995, Seismic velocity structure and composition of the continental crust: A global view: Journal of Geophysical Research, v. 100, no. B7, p. 9761–9788, doi: 10.1029/95JB00259.

Csejtey, B., Jr., Mullen, M.W., Cox, D.P., and Stricker, G.D., 1992, Geology and geochronology of the Healy quadrangle, south-central Alaska: U.S. Geological Survey Miscellaneous Investigations Series, Map I-1961, scale 1:250,000, 63 p.

Eberhart-Phillips, D., and 28 others, 2003, The 2002 Denali fault earthquake, Alaska: A large magnitude, slip-partitioned event: Science, v. 300, p. 1113–1118, doi: 10.1126/science.1082703.

England, P., and McKenzie, D., 1982, A thin viscous sheet model for continental deformation: Royal Astronomical Society Geophysical Journal, v. 70, p. 295–321.

Ferris, A., Abers, G.A., Christensen, D.H., and Veenstra, E., 2003, High resolution of the subducted Pacific (?) plate beneath central Alaska, 50–150 km depth: Earth and Planetary Science Letters, v. 214, p. 575–588, doi: 10.1016/S0012-821X(03)00403-5.

Fitzgerald, P.G., Sorkhabi, R.B., Redfield, T.F., and Stump, E., 1995, Uplift and denudation of the central Alaska Range: A case study in the use of apatite fission track thermochronology to determine absolute uplift parameters: Journal of Geophysical Research, v. 100, no. B10, p. 20,175–20,191, doi: 10.1029/95JB02150.

Kirschner, C.E., 1994, Interior basins of Alaska, *in* Plafker, G., and Berg, H.D., eds., The geology of Alaska: Boulder, Colorado, Geological Society of America, Geology of North America, v. G-1, p. 469–493.

Langston, C.A., 1979, Structure under Mount Rainier, Washington, inferred from teleseismic body waves: Journal of Geophysical Research, v. 84, no. B9, p. 4749–4762.

Ludwig, W.J., Nafe, J.E., and Drake, C.L., 1970, Seismic refraction, *in* Maxwell, A.E., ed., The sea, Volume 4: New York, Wiley-Interscience, p. 53–84.

Mann, P., and Frohlick, C., 1999, Classification and tectonic comparison of subduction to strike-slip transitions on active plate boundaries: Penrose Conference Abstract, p. 60–62: http://people.uncw.edu/grindlayn/revabstr_vol.pdf (May 2006).

McNamara, D.E., and Pasyanos, M.E., 2002, Seismological evidence for a sub-volcanic arc mantle wedge beneath the Denali volcanic gap, Alaska: Geophysical Research Letters, v. 29, doi: 10.1029/2001GL014088.

Melosh, H.J., and Raefsky, A., 1980, The dynamical origin of subduction zone topography: Royal Astronomical Society Geophysical Journal, v. 60, p. 333–354.

Meyers, E. Veenstra, Christensen, D.H., Abers, G.A., Stachnik, J.C., Holland, A.R., and Beebe, K.B., 2000, Broadband (seismic) Experiment Across the Alaska Range (BEAAR) to determine the crustal and upper mantle structure beneath central Alaska: Eos (Transactions, American Geophysical Union), Fall Meeting Supplement, v. 81, no. 48, abs. S72A–11, p. F877.

Meyers, E. Veenstra, Christensen, D.H., Ferris, A., Abers, G.A., and Lucier, A.M., 2001, Crustal thickness across the Alaska Range: Eos (Transactions, American Geophysical Union), Fall Meeting Supplement, v. 82, no. 47, abs. T41C-0907, p. F1204.

Meyers, E. Veenstra, Christensen, D.H., Abers, G.A., 2002, Moho topography beneath the Alaska Range: Eos (Transactions, American Geophysical Union), Fall Meeting Supplement, v. 83, no. 47, abs. S52A-1073, p. F968.

Nokleberg, W.J., Plafker, G., and Wilson, F.H., 1994, Geology of south-central Alaska, *in* Plafker, G., and Berg, H.D., eds., The geology of Alaska: Boulder, Colorado, Geological Society of America, Geology of North America, v. G-1, p. 311–366.

Owens, T.J., Zandt, G., and Taylor, S.R., 1984, Seismic evidence for an ancient rift beneath the Cumberland Plateau, Tennessee: A detailed analysis of broadband teleseismic P waveforms: Journal of Geophysical Research, v. 89, no. B9, p. 7783–7795.

Page, R.A., Plafker, G., Fuis, G.S., Nokleberg, W.J., Ambos, E.L., Mooney, W.D., and Campbell, D.L., 1986, Accretion and subduction tectonics in the Chugach Mountains and Copper River Basin, Alaska: Initial results of the Trans-Alaska Crustal Transect: Geology, v. 14, p. 501–505, doi: 10.1130/0091-7613(1986)14<501:AASTIT>2.0.CO;2.

Pavlis, T.L., Sisson, V.B., Foster, H.L., Nokleberg, W.J., and Plafker, G., 1993, Mid-Cretaceous extensional tectonics of the Yukon-Tanana terrane, Trans-Alaska Crustal Transect (TACT), east-central Alaska: Tectonics, v. 12, p. 103–122.

Plafker, G., and Berg, H.C., 1994, Overview of the geology and tectonic evolution of Alaska, *in* Plafker, G., and Berg, H.D., eds., The geology of Alaska: Boulder, Colorado, Geological Society of America, Geology of North America, v. G-1, p. 989–1021.

Sheehan, A.F., Abers, G.A., Jones, C.H., and Lerner-Lam, A.L., 1995, Crustal thickness variations across the Colorado Rocky Mountains from teleseismic receiver functions: Journal of Geophysical Research, v. 100, p. 20,391–20,404, doi: 10.1029/95JB01966.

Silberling, N.J., Jones, D.L., Monger, J.W.H., Coney, P.J., Berg, H.C., and Plafker, G., 1994, Lithotectonic terrane map of Alaska and adjacent parts of Canada, *in* Plafker, G., and Berg, H.D., eds., The geology of Alaska: Boulder, Colorado, Geological Society of America, Geology of North America, v. G-1, plate 3, scale 1:2,500,000.

Stachnik, J.C., Abers, G.A., and Christensen, D.H., 2004, Seismic attenuation and mantle wedge temperatures in the Alaska subduction zone: Journal of Geophysical Research, v. 109, no. B10, p. B10304, doi: 10.1029/2004JB003018.

Wessel, P., and Smith, W.H.F., 1995, New version of the generic mapping tools released: Eos (Transactions, American Geophysical Union), v. 76, p. 329.

Wolf, L.W., Stone, D.B., and Davies, J.N., 1991, Crustal structure of the active margin, south-central Alaska: An interpretation of seismic refraction data from the Trans-Alaska Crustal Transect: Journal of Geophysical Research, v. 96, no. B10, p. 16,455–16,469.

Zhao, D., Christensen, D.H., and Pulpan, H., 1995, Tomographic imaging of the Alaska subduction zone: Journal of Geophysical Research, v. 100, no. B4, p. 6487–6504, doi: 10.1029/95JB00046.

Zhu, L., and Helmberger, D.V., 1998, Moho offset across the northern margin of the Tibetan Plateau: Science, v. 281, p. 1170–1172, doi: 10.1126/science.281.5380.1170.

Manuscript received 18 January 2006
Revised manuscript received 18 April 2006
Manuscript accepted 1 May 2006

Printed in USA